Electron attachment to Cl_2 from 300 to 1100 K: Experiment and theory

Jeffrey F. Friedman,[1,*] Thomas M. Miller,[1,†] Linda C. Schaffer,[2] A. A. Viggiano,[1] and Ilya I. Fabrikant[3]
[1]*Space Vehicles Directorate, Air Force Research Laboratory, 29 Randolph Road, Hanscom Air Force Base, Massachusetts 01731-3010, USA*
[2]*College of Education, University of New Mexico, Albuquerque, New Mexico 87131, USA*
[3]*Department of Physics and Astronomy, University of Nebraska, Lincoln, Nebraska 68588-0111, USA*
(Received 31 December 2008; published 17 March 2009)

Rate constants for dissociative electron attachment to Cl_2 have been measured from 300 to 1100 K in a high-temperature flowing-afterglow Langmuir-probe apparatus. *R*-matrix calculations have been carried out which compare well with the present measurements with possible deviation at the highest temperatures. The attachment rate constants do not show Arrhenius behavior. The temperature dependence of the calculated rate constants for successive vibrational levels provides insight as to this behavior. While the lowest vibrational level of Cl_2 dominates attachment at low temperatures, the rate constant is not flat with temperature because of the *p*-wave character of the attachment process. The non-Arrhenius behavior is due to a conflict between the increase in attachment cross section with vibrational level (temperature) and the decline in the cross section with electron energy above 50 meV.

DOI: 10.1103/PhysRevA.79.032707 PACS number(s): 34.80.Ht, 34.10.+x, 52.20.Fs, 52.27.Cm

I. INTRODUCTION

Experience tells one that chlorine-containing molecules *M*Cl will attach zero-energy electrons efficiently, yielding Cl^- anions [1,2]. The reason is that the *M*-Cl bond energy is commonly smaller than the electron affinity of Cl [EA(Cl)] so that dissociative attachment is exothermic and the process results in a strong zero-energy resonance. So it is at first surprising that the chlorine molecule itself attaches electrons with only about 1% efficiency at 300 K, even though it is exothermic [3]. Until this decade Cl_2 presented an enigma because electron-beam experiments showed an attachment feature typical of zero-energy resonances, though weak, while electron capture into the lowest Cl_2^- electronic state requires a *p*-wave process,

$$e^- + Cl_2(X^1\Sigma_g^+) \rightarrow Cl_2^-(X^2\Sigma_u^+) \rightarrow Cl(^2P) + Cl^-(^1S). \quad (1)$$

The relevant negative-ion states involved were correctly identified by Azria *et al.* [4] in a 1982 experiment.

This situation was more uncertain for the analogous case of F_2 because the 1987 high-resolution (6 meV) data of Chutjian and Alajajian [5] were said to prove conclusively that *s*-wave attachment was occurring because the cross section σ fit the Wigner $\sigma \sim E^{-1/2}$ law appropriate for *s*-wave attachment as a function of electron energy *E*. It was argued that the higher-lying $^2\Sigma_g^+$ electronic state of F_2^- was mixing in nonadiabatically [5]. Another possibility suggested was that a *p*-wave threshold was hidden within the 6 meV resolution of the experiment [6].

The question for Cl_2 was resolved in Ref. [7]. Fabrikant *et al.* carried out *R*-matrix calculations for reaction (1) and found that the observed attachment resonance peaked not at zero energy but at 50 meV [7]. The cross section σ followed the Wigner *p*-wave threshold law, $\sigma \sim E^{1/2}$, in rising from zero energy but declined beyond 50 meV due to an unusual rapid decline in the Franck-Condon factor between anion and neutral, coupled with greater autodetachment probability for Cl_2^- with increasing electron energy. The resulting cross-section peak predicted to lie at 50 meV could easily be mistaken for a zero-energy resonance in experiments which typically have energy resolutions of 50 meV and higher. The cross sections were normalized to the drift tube measurements of McCorkle *et al.* [8] at 0.1 eV electron energy by adjusting an *R*-matrix parameter [7]. Thus normalized, the theoretical calculations compared well with the measurements of McCorkle *et al.* over an electron energy range of 46–800 meV and 213–323 K. Explicit verification of the Fabrikant *et al.* calculations and normalization choice came from high-resolution (1 meV) experiments by Barsotti *et al.* [9] and Ruf *et al.* [10]. In the latter work, the *R*-matrix cross sections were argued to be treated as the recommended values for future work and applications, replacing those recommended in the reviews by Christophorou and Olthoff [3,11]. The *R*-matrix calculations were also extended to show the vibrational state dependence of the attachment rate constant and to include higher-energy resonances due to electronic excitation of Cl_2^- [10]. Earlier work on Cl_2 was covered in Refs. [3,9–13], notably the measurements at Birmingham University (UK), which provided attachment rate constants from 205 to 590 K [13].

Experiments from the Kaiserslautern group [14] recently provided high-resolution (1-meV) data for F_2 which clearly show a *p*-wave shape resonance for attachment through the F_2^- (Σ_u^+) ground state, with a peak at 31 meV, in contrast to older work [5]. However, the *R*-matrix theory that was so successful for Cl_2 failed to properly describe attachment to F_2. *R*-matrix calculations with available F_2^- potential-energy curves [15–18] result in the peak position at 170 meV, consistent with previous dissociative attachment calculations [17]. Attempts to modify the anion curves to make the peak position consistent with the measurements [14] resulted in unrealistic potential curves and very small attachment rate

*Permanent address: Department of Physics, University of Puerto Rico, Mayaguez, Puerto Rico 00681.
†Also at Institute for Scientific Research, Boston College, Chestnut Hill, Massachusetts 02167.

constants that were inconsistent with drift tube measurements [19].

In the present work we have used a different high-temperature flowing-afterglow Langmuir-probe (HT-FALP) apparatus to measure reaction-rate constants from 300 to 1100 K. In addition, the *R*-matrix formulation of the problem has been used to calculate thermal rate constants over the same temperature range. The results confirm the striking, and non-Arrhenius, vibrational energy dependence predicted by the *R*-matrix calculations.

A note on energetics: the experimental bond dissociation energy of Cl_2 is 2.51 ± 0.02 eV at 298 K [20], and the experimental electron affinity of Cl is EA(Cl) $=3.612\,724 \pm 0.000\,027$ eV [21]. Ignoring the 0 vs 298 K difference in these two quantities, the exothermicity for reaction (1) is 1.10 eV. The parent anion is not observed in low-pressure electron attachment experiments. Christophorou and Olthoff [3] recommended EA(Cl_2)=2.45 eV from a review of experimental data.

II. EXPERIMENT

The present HT-FALP apparatus has recently been described in detail, so only a cursory outline will be given here [22]. A weak He^+, Ar^+ plasma is created in a microwave discharge cavity, through which a He buffer gas flows, with a few percent of Ar added following the discharge. The gas pressure in the flow tube was 130 Pa at 300 K and up to 370 Pa at higher temperatures. The plasma enters the preheating zone of a 7-cm internal diameter (ID) quartz flow tube of about 1-m length. Halfway down this length, the buffer gas enters a constant-temperature reaction zone. A few ppm by volume of Cl_2 gas is injected into the flow tube at this point through a toroidal inlet with four hollow needles facing radially to distribute the Cl_2 uniformly across the flow tube cross section. Plasma electrons attach to the Cl_2 downstream of the inlet, and the electron density along the flow tube axis is measured with a movable, cylindrical, Langmuir probe. If there was no diffusive loss of electrons, the attachment loss would follow an exponential decay with distance (time) along the flow tube, and the attachment rate constant could be determined from the decay constant and the measured plasma velocity. However, ambipolar diffusion is not negligible, so the diffusion frequency ν_D must first be measured in absence of Cl_2. The observed decay of electron density n_e in the presence of Cl_2 is then due to the coupled effects of diffusion and attachment according to

$$n_e = n_e(0)[\nu_a \exp(-\nu_a t) - \nu_D \exp(-\nu_D t)]/(\nu_a - \nu_D), \quad (2)$$

where $n_e(0)$ is the electron density at time $t=0$ and ν_a is the attachment frequency, related to the attachment rate constant k_a by $\nu_a = k_a n_r$, with n_r as the reactant (Cl_2) concentration [2,23]. The relevant rate equations leading to solution (2) were given in Ref. [22]. Sample data obtained at 1008 K for Cl_2 are given in Fig. 1. In cases where k_a is very small ($\sim 10^{-11}$ cm^3 s^{-1}), a correction for loss due to electron-ion recombination may be needed, as shown in Ref. [22]. The Cl_2 attachment rate constants are large enough such that no such correction is needed.

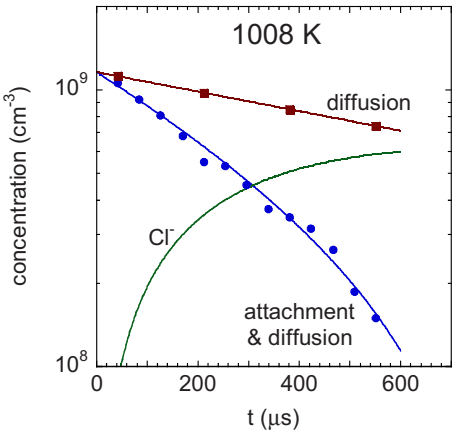

FIG. 1. (Color online) HT-FALP data for electron attachment to Cl_2 at 1008 K, obtained in a He/Ar buffer gas of pressure 333 Pa (2.39×10^{16} cm^{-3}). The diffusion data were obtained in the absence of Cl_2, while the attachment data were obtained with 2.69×10^{11} cm^{-3} Cl_2. The solid curves are solutions to the rate equations given in Ref. [22]; see Eq. (2).

Two issues arose with high-temperature operation that deserve note and are described more thoroughly in Ref. [22]. One is that ambipolar diffusion loss of electrons becomes more important at high temperatures. A large diffusive loss is a problem not only because of competition with attachment but also because it can be severe enough that the electron density at the reactant inlet is too low [$n_e(0) \approx 5 \times 10^8$ cm^{-3}] to allow attachment measurements to be made with the Langmuir probe for a full decade of decay in n_e. We combat the diffusive loss by increasing the buffer gas flow rate (hence, the gas velocity through the flow tube) and by increasing the fraction of argon gas (the diffusion rate is lower in Ar than in He). Since the Ar fraction increased with temperature, from 2% at 300 K to 13% at 1100 K, the behavior of the diffusion coefficients are not useful aside from use in Eq. (2). We plan to do a systematic study of the temperature dependence of the diffusion coefficient sometime in the future.

The second issue is that above 900 K the Langmuir-probe current-voltage characteristics become distorted on the positive-ion side (negative potentials). They appear normal on the electron side (positive potentials) aside from what appears to be a small leakage current added to the baseline of the characteristic. Examples were shown in Ref. [22]. Because the electron currents to the probe follow the expected parabolic shape with bias potential, we have continued to interpret these straightforwardly in terms of n_e even though we do not yet understand the positive-ion distortions. Further, the measured diffusive loss follows the expected exponential behavior along the flow tube axis. We note that even at room-temperature positive-ion collection by cylindrical probes is not easily interpreted because of collisions with buffer gas atoms in the plasma sheath around the Langmuir probe [24–27].

Our Cl_2 sample was purchased from the Sigma-Aldrich Co. with a purity of $\geq$99.5% and was used as supplied. The major impurities are nonattaching gases (at our pressures), CO_2, N_2, and O_2. Traces of chlorinated hydrocarbons and

ferric chloride may be present due to reaction with transfer tubing and storage cylinders. Traces of Br_2 and/or I_2 may be present, depending on the purity of the salts used in the manufacture of Cl_2. Our mass spectrum showed no anions other than Cl^- which could be attributed to impurities, except for trace anions (e.g., O^- and NO_2^-) created from air impurities that enter from a vacuum box surrounding the flow tube and furnace. Material problems relating to high temperatures leave us with imperfect seals around the flow tube [22].

The accuracy of the HT-FALP data is thought to be ±25% in the temperature range 300–900 K and ±30% for temperatures >900 K because of the Langmuir-probe issue discussed above. The relative accuracy between points at different temperatures is estimated to be ±15% at temperatures less than 900 K and ±20% at higher temperatures [22].

III. THEORY

The calculations reported here are an extension of those reported earlier, applied to the higher temperatures of the present experiment [7,10]. A one-pole approximation for the *R*-matrix was used,

$$R = R_b + \gamma^2(\rho)/[W(\rho) - E], \tag{3}$$

where ρ is the internuclear separation, R_b is a background term weakly dependent on ρ, $\gamma(\rho)$ is the surface amplitude, $W(\rho)$ is the lowest *R*-matrix pole, and E is the electron energy. The one-pole approximation is equivalent to the inclusion of one term in the resonance Breit-Wigner formula. This formulation allowed adjustment of $\gamma(\rho)$ to match the experimental value of the attachment cross section. The measured attachment cross section of McCorkle *et al.* [8] at 0.1 eV was chosen for this purpose. As noted above, the high-resolution experiments of Barsotti *et al.* [9] and Ruf *et al.* [10] showed this choice to be a good one. More recent *ab initio* calculations [28] confirm the existence of the low-energy peak in the dissociative attachment cross section, albeit at somewhat higher energy. In addition, the cross section calculated in Ref. [28] decays more slowly at higher energies than found in Ref. [7]. The cross sections grow with the vibrational quantum number ν, but this growth is somewhat slower than calculated in Ref. [10]. We attribute these differences to different shapes of anion potential-energy curves used in the calculations. The anion curve used in Refs. [7,10] crosses the neutral farther to the left from the equilibrium internuclear separation and positioned much closer to the neutral curve to the left of the crossing point than in Ref. [28].

Rotational effects in dissociative attachment to Cl_2 were found much less important than vibrational effects [28]. Since the electron energies involved are large compared to the rotational spacing, the approximation of fixed molecular orientation used in the present calculations is adequate.

IV. RESULTS

Experimental and theoretical rate constants for electron attachment to Cl_2 are given in Table I and plotted in Fig. 2.

TABLE I. Experimental and theoretical rate constants (in units of 10^{-9} cm^3 s^{-1}) versus temperature for electron attachment to Cl_2. The uncertainty for the present experimental data is ±25% except ±30% above 900 K. The stated uncertainty for the experiment of McCorkle *et al.* is ±10%, for Smith *et al.* it is ±15% (first two data) and ±20% (final two data), and for Ayala *et al.* it is ±14%.

Present		Present		McCorkle *et al.*		Smith *et al.*		Ayala *et al.*	
T (K)	Theory	*T* (K)	Expt.	*T* (K)	Ref. [8]	*T* (K)	Ref. [13]	*T* (K)	Ref. [29]
200	1.14	292	1.6	213	1.22	203	<1.0	300	0.29
250	1.38	352	2.0	233	1.35	300	2.0	300	0.27
300	1.64	400	2.2	253	1.51	455	3.3	300	0.28
350	1.93	500	2.7	273	1.67	590	4.8	311	0.24
400	2.33	650	3.0	298	1.86			330	0.33
500	2.88	750	2.9	323	2.14			353	0.31
600	3.56	844	5.7					374	0.34
700	4.23	1008	6.7					394	0.35
800	4.85	1103	9.0					413	0.37
900	5.42							434	0.43
1000	5.90							454	0.40
1100	6.43							476	0.45
								503	0.54
								520	0.54
								544	0.54
								561	0.49
								581	0.47
								603	0.56
								603	0.54

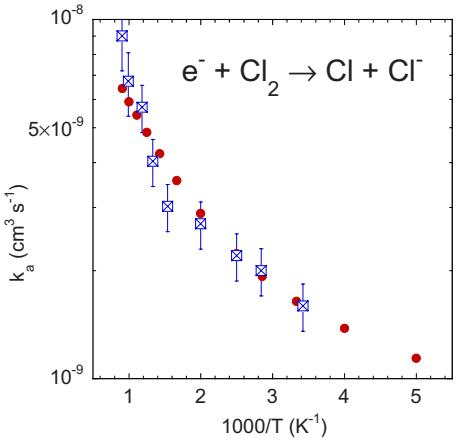

FIG. 2. (Color online) *R*-matrix (solid circles) and present experimental (squares with error bars) rate constants for electron attachment to Cl_2, 200–1100 K. The error bars indicate estimated ±15% relative uncertainties (±20% above 900 K).

The experimental numbers are the average of data obtained with two different concentrations of Cl_2. The error bars in Fig. 2 represent the estimated relative uncertainty in the experimental data, ±15% (±20% for $T>900$ K). The agreement is generally quite good though there is an increasing small systematic discrepancy at the highest temperatures, with the calculated value at 1100 K, lying 29% lower than the experimental datum. Still, the non-Arrhenius behavior is clear. The main reason for the rapid increase in k_a with temperature was shown by Ruf *et al.* [10] in that the attachment cross section increased dramatically with increasing vibrational excitation. The dependence on vibrational level is illustrated in Fig. 3(a), where the calculated rate constants for $\nu=0$ through $\nu=7$ are plotted vs temperature. The rate constants increase substantially with increasing excitation by a factor of 4 for $\nu=1$, a factor of 9 for $\nu=2$, and with $\nu=7$ being 19 times faster than $\nu=0$ in the middle of our temperature range. The increasing portion of the rate constant curves in Fig. 3(a) is due to the Wigner threshold law and the decrease results from Franck-Condon factors.

Figure 3(b) shows the fractional population of each level as a function of temperature. At all temperatures relevant to this study, the ground level is most highly populated. Only above 1000 K does the $\nu=3$ population rise above 10% that of $\nu=0$. However, since the partial rate constants increase so dramatically with vibrational level, the higher levels make a significant contribution to the total rate constant. Figure 3(c) shows the contribution to the total rate constant from each vibrational level, i.e., the curves in Fig. 3(a) are multiplied by the populations shown in Fig. 3(b). At 300 K, the total rate constant is dominated by the $\nu=0$ partial rate constant. By 550 K, the contribution from $\nu=1$ is shown to be the most important contributor to the total rate constant, and the $\nu=2$ partial rate constant becomes dominant near 950 K.

In Fig. 4 we added the attachment data from the 1980s to the plot given in Fig. 2, and the numbers are tabulated in Table I. The Oak Ridge National Laboratory (ORNL) data of McCorkle *et al.* [8] were obtained using a drift tube apparatus with a N_2 buffer gas at pressures of 3–8 atm. The University of Birmingham data were obtained using a FALP apparatus with a He/Ar buffer gas at pressures of 65–130 Pa [13]. The University of Houston data were obtained using an electron-capture detector with an Ar/CH_4 buffer gas, apparently at atmospheric pressure [29]. We had to multiply the Houston data by a factor of 6.2 to get them on the graph in Fig. 4. Once done, one sees that the shape of the data vs temperature fits the trend of the present work. See the book by Christophorou and Olthoff [3], a review article by Hotop *et al.* [12], and the paper by Ruf *et al.* [10] for comments on all previous measurements of attachment cross sections and rate constants for Cl_2, including several measured only at 300 K [3,29].

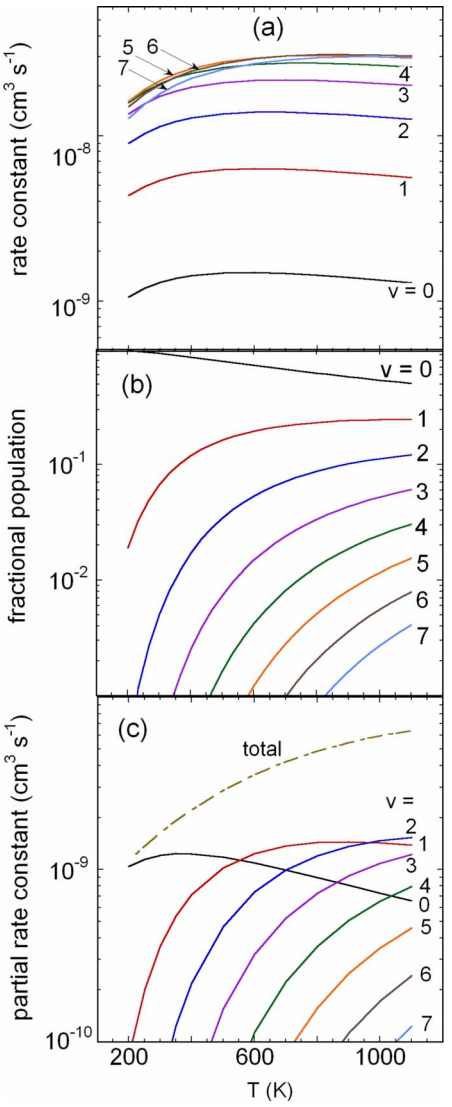

FIG. 3. (Color online) (a) Rate constants for electron attachment to Cl_2 for $\nu=0-7$. (3) Fractional populations of $\nu=0-7$ vs temperature. (3) Partial rate constants for $\nu=0-7$ [product of numbers in (a) and (b)] and the total rate constant.

Deviations from Arrhenius behavior were discussed in Ref. [30] but mostly for *s*-wave attachment. For *s*-wave attachment at low temperatures the rate constant turns to a nearly constant value which basically reflects the rate coefficient for the $\nu=0$ vibrational level. From Fig. 3(c), it is

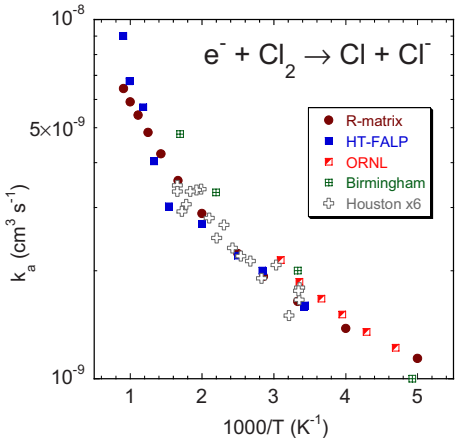

FIG. 4. (Color online) Present results (*R* matrix and HT-FALP) compared to Oak Ridge National Laboratory drift tube data (Ref. [8]) (213–323 K), Birmingham FALP data (Ref. [13]) (203–590 K), and Houston electron-capture detector data multiplied by a factor of 6.2 (Ref. [29]) (300–600 K).

clear that for attachment to Cl_2, $\nu=0$ also dominates at low temperatures. However, in contrast to the *s*-wave attachment, the *p*-wave attachment cross section is proportional to $E^{1/2}$ and the rate constant proportional to T. Therefore, the temperature dependence in the low-temperature limit is not flat for the *p*-wave case nor does it exhibit Arrhenius behavior typical of high temperatures. In fact, the temperature dependence in the low-energy region is substantially weaker than the Wigner Law implies because the $E^{1/2}$ dependence of the cross section holds only in the very low-energy region below about 15 meV [10]. The overall shape of the curve is then determined by the factors shown in Figs. 3(a) and 3(b).

V. SUMMARY

Dissociative attachment rate constants have been measured from 300 to 1100 K with a high-temperature flowing-afterglow Langmuir-probe apparatus. *R*-matrix calculations of the rate constants have been extended to 1100 K. Experiment and theory agree well with possible departure at the highest temperatures. The rate constants display non-Arrhenius behavior because of the unusual shape of the *p*-wave attachment cross section with electron energy, which peaks at 50 meV, and show a strong vibrational energy dependence.

ACKNOWLEDGMENTS

We are grateful for the support of the Air Force Office of Scientific Research for this work. T.M.M. is under contract (Grant No. FA8718-04-C0006) to the Institute for Scientific Research of Boston College. J.F.F. was supported by the Air Force Research Laboratory Summer Faculty Program. I.I.F. was supported by the U.S. National Science Foundation under Grant No. PHY-0652866.

[1] L. G. Christophorou, D. L. McCorkle, and A. A. Christodoulides, in *Electron-molecule Interactions and Their Applications*, edited by L. G. Christophorou (Academic, New York, 1984), pp. 477–617.
[2] D. Smith and P. Španěl, Adv. At., Mol., Opt. Phys. **32**, 307 (1994).
[3] L. G. Christophorou and J. K. Olthoff, *Fundamental Electron Interactions with Plasma Processing Gases* (Kluwer Academic, New York, 2004).
[4] R. Azria, R. Abouaf, and D. Teillet-Billy, J. Phys. B **15**, L569 (1982).
[5] A. Chutjian and S. H. Alajajian, Phys. Rev. A **35**, 4512 (1987).
[6] A. Chutjian, A. Garscadden, and J. M. Wadehra, Phys. Rep. **264**, 393 (1996).
[7] I. I. Fabrikant, T. Leininger, and F. X. Gadéa, J. Phys. B **33**, 4575 (2000).
[8] D. L. McCorkle, A. A. Christodoulides, and L. G. Christophorou, Chem. Phys. Lett. **109**, 276 (1984).
[9] S. Barsotti, M.-W. Ruf, and H. Hotop, Phys. Rev. Lett. **89**, 083201 (2002).
[10] M.-W. Ruf, S. Barsotti, M. Braun, H. Hotop, and I. I. Fabrikant, J. Phys. B **37**, 41 (2004).
[11] L. G. Christophorou and J. K. Olthoff, J. Phys. Chem. Ref. Data **29**, 267 (2000).
[12] H. Hotop, M.-W. Ruf, M. Allan, and I. I. Fabrikant, Adv. At., Mol., Opt. Phys. **49**, 85 (2003).
[13] D. Smith, N. G. Adams, and E. Alge, J. Phys. B **17**, 461 (1984).
[14] M. Braun, M.-W. Ruf, I. I. Fabrikant, and H. Hotop, Phys. Rev. Lett. **99**, 253202 (2007).
[15] A. U. Hazi, A. E. Orel, and T. N. Rescigno, Phys. Rev. Lett. **46**, 918 (1981).
[16] J. N. Bardsley and J. M. Wadehra, J. Chem. Phys. **78**, 7227 (1983).
[17] V. Brems, T. Beyer, B. M. Nestmann, H.-D. Meyer, and L. S. Cederbaum, J. Chem. Phys. **117**, 10635 (2002).
[18] M. Ingr, H.-D. Meyer, and L. S. Cederbaum, J. Phys. B **32**, L547 (1999).
[19] D. L. McCorkle, L. G. Christophorou, A. A. Christodoulides, and L. Pichiarella, J. Chem. Phys. **85**, 1966 (1986).
[20] *Handbook of Chemistry and Physics*, 88th ed., edited by D. R. Lide (CRC Press, Boca Raton, FL, 2007), p. 57.
[21] U. Berzinsh, M. Gustafsson, D. Hanstorp, A. Klinkmüller, U. Ljungblad, and A.-M. Mårtensson-Pendrill, Phys. Rev. A **51**, 231 (1995).
[22] T. M. Miller, J. F. Friedman, J. S. Williamson, L. C. Schaffer, and A. A. Viggiano, Rev. Sci. Instrum. (to be published).
[23] T. M. Miller, Adv. At., Mol., Opt. Phys. **51**, 299 (2005).
[24] D. Smith and I. C. Plumb, J. Phys. D **6**, 196 (1973).
[25] D. Trunec, P. Španěl, and D. Smith, Contrib. Plasma Phys. **35**, 203 (1995).
[26] P. Španěl, D. Smith, O. Chudacek, P. Kudrna, and M. Tichy, Contrib. Plasma Phys. **35**, 3 (1995).
[27] R. Johnsen, E. V. Shun'ko, T. Gougousi, and M. F. Golde,

Phys. Rev. E **50**, 3994 (1994).
[28] P. Kolorenč and J. Horáček, Phys. Rev. A **74**, 062703 (2006).
[29] J. A. Ayala, W. E. Wentworth, and E. C. M. Chen, J. Phys. Chem. **85**, 768 (1981). We converted the intermediate quantity k_1' plotted in Fig. 3 of this paper to attachment rate constants k_1 using Eqs. 22–27 and the reported 300 K result of $2.8 \pm 0.4 \times 10^{-10}$ cm^3 s^{-1} and Arrhenius activation energy of 370 ± 4 meV.
[30] I. I. Fabrikant and H. Hotop, J. Chem. Phys. **128**, 124308 (2008).